Dear Author

Please use this PDF proof to check the layout of your article. If you would like any changes to be made to the layout, you can leave instructions in the online proofing interface. First, return to the online proofing interface by clicking "Edit" at the top page, then insert a Comment in the relevant location. Making your changes directly in the online proofing interface is the quickest, easiest way to correct and submit your proof.

Please note that changes made to the article in the online proofing interface will be added to the article before publication, but are not reflected in this PDF proof.

If you would prefer to submit your corrections by annotating the PDF proof, please download and submit an annotatable PDF proof by clicking the link below.

Annotate PDF

Article

Current Biology

Functional organization of visual responses in the octopus optic lobe

Graphical abstract

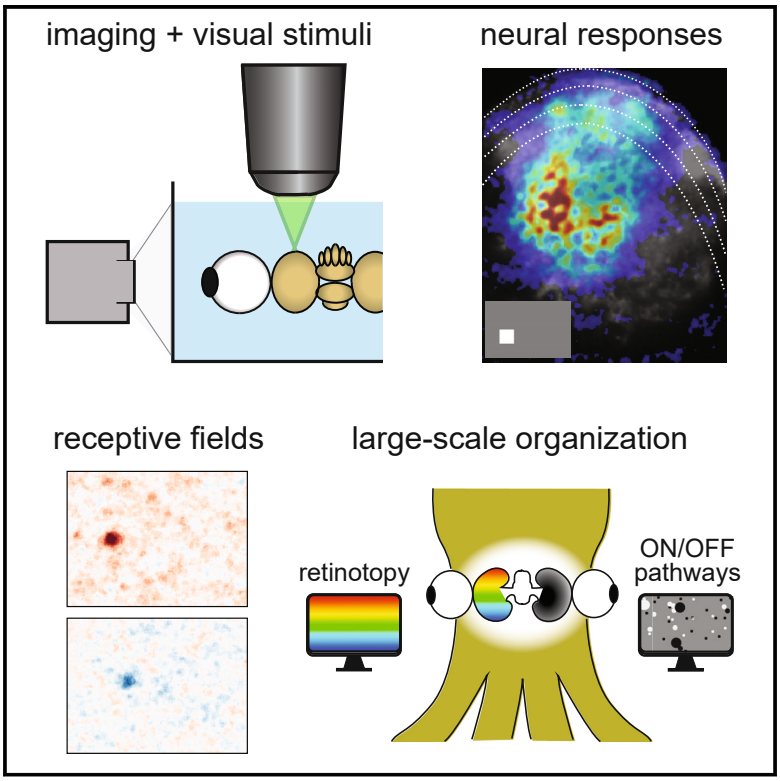

Authors

Judit R. Pungor, V. Angelique Allen, Jeremea O. Songco-Casey, Cristopher M. Niell

Correspondence

jpungor@uoregon.edu (J.R.P.), cniell@uoregon.edu (C.M.N.)

In brief

Pungor et al. use calcium imaging to measure visually evoked response properties in the cephalopod central nervous system. They demonstrate shared and novel aspects of visual function in the octopus, including retinotopic organization, the emergence of ON and OFF pathways, and asymmetries in the processing of light and dark stimuli.

Highlights

- The functional organization of the cephalopod visual system is largely unknown
- Using calcium imaging, we mapped visually evoked responses in the octopus optic lobe
- We identified spatially localized receptive fields with retinotopic organization
- ON and OFF pathways were distinct and had unique size selectivity properties

Pungor et al., 2023, Current Biology *33*, 1–10
July 10, 2023
https://doi.org/10.1016/j.cub.2023.05.069

CellPress

Please cite this article in press as: Pungor et al., Functional organization of visual responses in the octopus optic lobe, Current Biology (2023), https://doi.org/10.1016/j.cub.2023.05.069

Current Biology

CellPress
OPEN ACCESS

Article

Functional organization of visual responses in the octopus optic lobe

Q1 Judit R. Pungor,[1,*] V. Angelique Allen,[1] Jeremea O. Songco-Casey,[1] and Cristopher M. Niell[1,2,3,*]
[1]Department of Biology and Institute of Neuroscience, University of Oregon, Eugene, OR 97405, USA
[2]Twitter: @cris_niell
[3]Lead contact
*Correspondence: jpungor@uoregon.edu (J.R.P.), cniell@uoregon.edu (C.M.N.)
https://doi.org/10.1016/j.cub.2023.05.069

SUMMARY

Cephalopods are highly visual animals with camera-type eyes, large brains, and a rich repertoire of visually guided behaviors. However, the cephalopod brain evolved independently from those of other highly visual species, such as vertebrates; therefore, the neural circuits that process sensory information are profoundly different. It is largely unknown how their powerful but unique visual system functions, as there have been no direct neural measurements of visual responses in the cephalopod brain. In this study, we used two-photon calcium imaging to record visually evoked responses in the primary visual processing center of the octopus central brain, the optic lobe, to determine how basic features of the visual scene are represented and organized. We found spatially localized receptive fields for light (ON) and dark (OFF) stimuli, which were retinotopically organized across the optic lobe, demonstrating a hallmark of visual system organization shared across many species. An examination of these responses revealed transformations of the visual representation across the layers of the optic lobe, including the emergence of the OFF pathway and increased size selectivity. We also identified asymmetries in the spatial processing of ON and OFF stimuli, which suggest unique circuit mechanisms for form processing that may have evolved to suit the specific demands of processing an underwater visual scene. This study provides insight into the neural processing and functional organization of the octopus visual system, highlighting both shared and unique aspects, and lays a foundation for future studies of the neural circuits that mediate visual processing and behavior in cephalopods.

Q4 Q3 Q2 Q5 INTRODUCTION

Cephalopods evolved large and complex brains independently from the rest of the animal kingdom. Like vertebrates, cephalopods also evolved camera-type eyes that focus a high-resolution image onto a retina.[1] Together, their large brain and camera-type eyes implement a sophisticated visual system, which mediates a wide range of advanced visually based behaviors,[2] including prey capture and predator avoidance,[3,4] identifying mates,[5,6] spatial navigation,[7,8] and a remarkable ability to rapidly camouflage to their surroundings.[9–12] However, because the cephalopod brain evolved independently from that of other highly visual species, the neural organization of their visual system is dramatically different.

Anatomical studies have delineated the morphology and structural connectivity of neurons in the cephalopod retina and optic lobes.[13–20] Unlike the retina in vertebrates, the cephalopod retina contains only photoreceptors, which send axons out of the retina into the optic lobes of the brain (Figures 1A and 1C). The optic lobes comprise roughly two-thirds of the centralized nervous system and are where most of the visual processing in the cephalopod brain is thought to occur.[12] The outer optic lobe is a layered structure (Figures 1D and 1E), with two cell body layers, termed the outer granular (OGL) and inner granular layer (IGL), surrounding a layer of processes, the plexiform layer (Plex), where photoreceptor axons terminate. Together, these were termed the "deep retina" due to their resemblance to the layers of the vertebrate retina.[13,15] The center of the optic lobe, the medulla (Med), consists of clusters of cell bodies arranged in a tree-like structure surrounded by neuropil.[21] Recent transcriptomic studies have revealed a rich diversity of cell types within the optic lobe, as well as extensive sub-laminar organization.[22–25]

Early studies of photoreceptors in the cephalopod eye provided an initial description of visual processing at the input stage.[26,27] Like most other invertebrates,[28] cephalopods have rhabdomeric photoreceptors that depolarize in response to increases in light (ON responses),[29] in contrast to vertebrate photoreceptors that depolarize in response to decrements in light (OFF responses). Nearly all species of cephalopods, including octopuses, only express one type of opsin in their photoreceptors and are therefore thought to be monochromats,[26,30] consistent with behavioral findings.[31,32] Electrophysiological recordings from the retina have demonstrated ON-center receptive fields (RFs) and indications of lateral inhibition.[33–36] However, little is known regarding neural responses beyond the photoreceptors.[35,37,38]

In the visual system of many species, responses to increments and decrements of light are processed in separate ON and OFF

Please cite this article in press as: Pungor et al., Functional organization of visual responses in the octopus optic lobe, Current Biology (2023), https://doi.org/10.1016/j.cub.2023.05.069

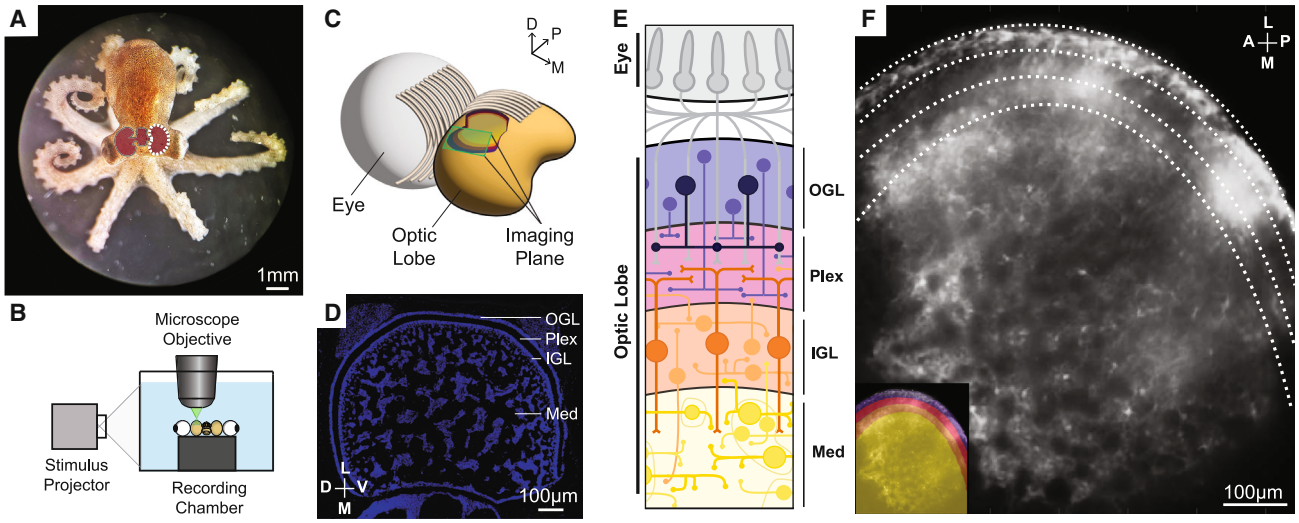

Figure 1. Experimental paradigm for the calcium imaging of visual responses in the optic lobe

(A) Image of a juvenile *Octopus bimaculoides*. The central brain is shown in burgundy, and one optic lobe is outlined in white.

(B) Schematic of the experimental set-up. A projector is used to present visual stimuli on the side of the recording chamber, with the preparation underneath the objective of a two-photon microscope on an adjustable platform.

(C) Illustration of octopus visual system anatomy. Bundles of photoreceptor projections exit the back of the eye (left), decussate vertically, and enter the optic lobe (right) in a retinotopic manner. In the cutaway, the layered structure of the optic lobe can be seen, as it is in our imaging planes. Dorsal, posterior, and medial axes are shown in the key.

(D) Coronal section of the center of the octopus optic lobe, stained with DAPI to illustrate the overall anatomy of the layers, which are labeled as in (E). Dorsal-ventral and lateral-medial axes are shown in the key.

(E) Simplified illustration of the anatomy of the layers of the optic lobe. Color code for layers also applies to (C) and (F).

(F) Mean fluorescence image of calcium indicator loading across a horizontal optical section of the optic lobe, as shown in the green square in (C), with layers delineated by dotted lines. Inset shows layers in color overlay. Lateral-medial and anterior-posterior axes are shown in the key.

pathways,[39] although the neural circuit mechanisms that give rise to these pathways, as well as their functional properties, can vary.[40,41] Likewise, many visual systems, though not all,[42] exhibit a topographic organization of visual space within the brain, known as retinotopy. However, no studies have addressed the neural representation of ON and OFF visual stimuli within the cephalopod optic lobe, or how this is organized topographically and transformed across the optic lobe layers.

Here, we developed techniques for two-photon calcium imaging of visually evoked responses in *Octopus bimaculoides*,[43] a promising model species for studying cephalopod vision.[44] We used this calcium imaging approach to measure how spatial and luminance information are represented in large-scale neural responses and to determine how these responses are organized within the optic lobe.

RESULTS

Calcium imaging of stimulus-specific visual responses in the optic lobe

Historically, electrophysiological recordings in the cephalopod brain have been technically challenging, and methods to express genetically encoded calcium indicators are not yet available in cephalopods. Here, we employed a calcium imaging approach using an injection of a synthetic calcium indicator, Cal-520 AM-ester, to measure large-scale neural activity in the octopus optic lobe. Our general approach was adapted from techniques previously used to measure visual responses in the zebrafish optic tectum[45] and the bolus-loading method established for acetoxymethyl (AM) ester calcium indicators.[46] In this method, a membrane-permeable AM-ester form of a calcium indicator dye is injected into the brain, where it is taken up by cells and rendered fluorescent based on cleavage of the AM moiety by endogenous esterases. This typically leads to dye loading across a region of 500–1,000 μm in the intact brain in zebrafish and mouse.[46]

We injected Cal-520 AM-ester into one optic lobe of an *ex vivo* preparation comprising the eyes and central brain of an octopus (Figure 1A) and imaged neural responses with a two-photon microscope, which provided optical access for recording across the optic lobe to a depth of up to 200 μm (Figure 1B). The small sizes of the juvenile octopuses allowed us to image a large cross-section of their optic lobes spanning multiple layers, providing a view across both its tangential and laminar organization (Figures 1C–1E), similar to how a cross-section of the top of the earth would both span longitude and latitude (tangential organization) as well as reveal the layers of the earth's crust and mantle (laminar organization). Figure 1F shows loading of the fluorescent indicator across an optic lobe, with its different layers readily discernible. The full field of view of the microscope was 0.64 mm^2, but measurable fluorescent loading typically only covered 0.35 ± 0.05 mm^2 (n = 6 animals). The radius of the optic lobe at this age is roughly 1 mm, with an approximately 4 mm^2 surface area, indicating we were imaging ~1/10th of the optic lobe area in a given experiment.

Visual stimuli were displayed via an LCD projector onto a white diffusion filter mounted on the side of the chamber containing the

Please cite this article in press as: Pungor et al., Functional organization of visual responses in the octopus optic lobe, Current Biology (2023), https://doi.org/10.1016/j.cub.2023.05.069

CellPress
OPEN ACCESS

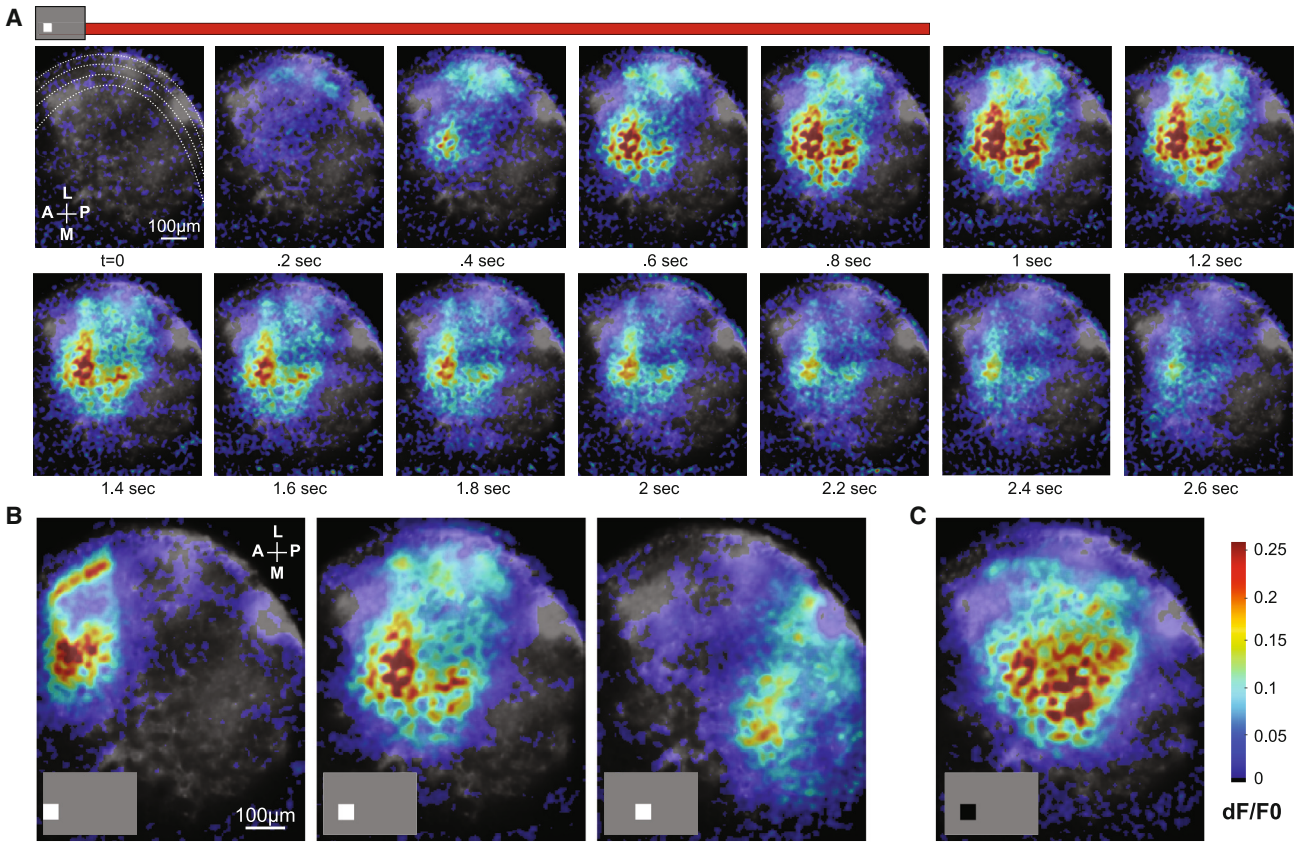

Figure 2. Visually evoked responses in the optic lobe

(A) Mean time course of fluorescence response to a flashed ON spot at one location in the visual field (averaged over five stimulus repetitions), showing spatial organization and temporal dynamics. Duration of stimulus presentation is indicated by the red bar above the frames. Individual imaging frames are shown at 0.2-s intervals.

(B) Mean fluorescence response across the optic lobe to ON stimuli at three different horizontal locations, averaged across the stimulus duration for five repetitions.

Q9 (C) Mean fluorescence response to an OFF stimulus at the same location as (H, middle), averaged across the stimulus duration for five repetitions.

See also Video S1.

preparation (Figure 1B). An adjustable platform allowed us to align the precise orientation of the eye so that RFs for a given imaging region were centered on the screen. This approach allowed us to present high-resolution stimuli across the visual field of one eye while simultaneously recording the responses across a region of the optic lobe.

To obtain visually evoked responses, we initially used a stimulus of individual full contrast ON (light) and OFF (dark) rectangular spots (24 × 18 deg) tiling the projection screen, presented in a random order on a 50% luminance gray background for 1 s duration. This stimulus elicited fluorescence responses in the optic lobe, dependent on the location of the spot in the visual field (Figure 2; Video S1). ON and OFF responses were based directly on the activity during the stimulus duration for light and dark spots, rather than comparing onset and offset transients for ON stimuli, as is done when light stimuli are presented on a dark background. Figure 2A shows the mean response, measured as the change in fluorescence divided by mean fluorescence (dF/F0) at each pixel across the optic lobe, over five repeated presentations of an ON spot at one location. The evoked activity, locked to stimulus onset, persisted throughout the 1-s stimulus period and was followed by a decay, consistent with calcium indicator dynamics. This activation map also suggests a temporal sequence of activity, with fluorescence signal first increasing rapidly in the superficial optic lobe, followed by a more gradual and sustained response in the Med. Figure 2B shows the mean response across the optic lobe during the stimulus presentation for ON spots in three neighboring locations. We found activation of distinct regions within the optic lobe to each location, indicating specificity for the location of the stimulus in visual space in a retinotopic manner. Finally, Figure 2C shows the response to an OFF spot at the same recording location as Figure 2B (middle), responding in approximately the same region, but deeper in the laminar structure of the optic lobe, in the IGL and Med.

These results demonstrate that our calcium imaging approach allowed us to measure stimulus-specific visual responses and provide initial support for both retinotopic and laminar organization of responses. To probe the specificity and spatial organization of visual responses more systematically, we next performed mapping of spatial RFs using a sparse noise stimulus.

Please cite this article in press as: Pungor et al., Functional organization of visual responses in the octopus optic lobe, Current Biology (2023), https://doi.org/10.1016/j.cub.2023.05.069

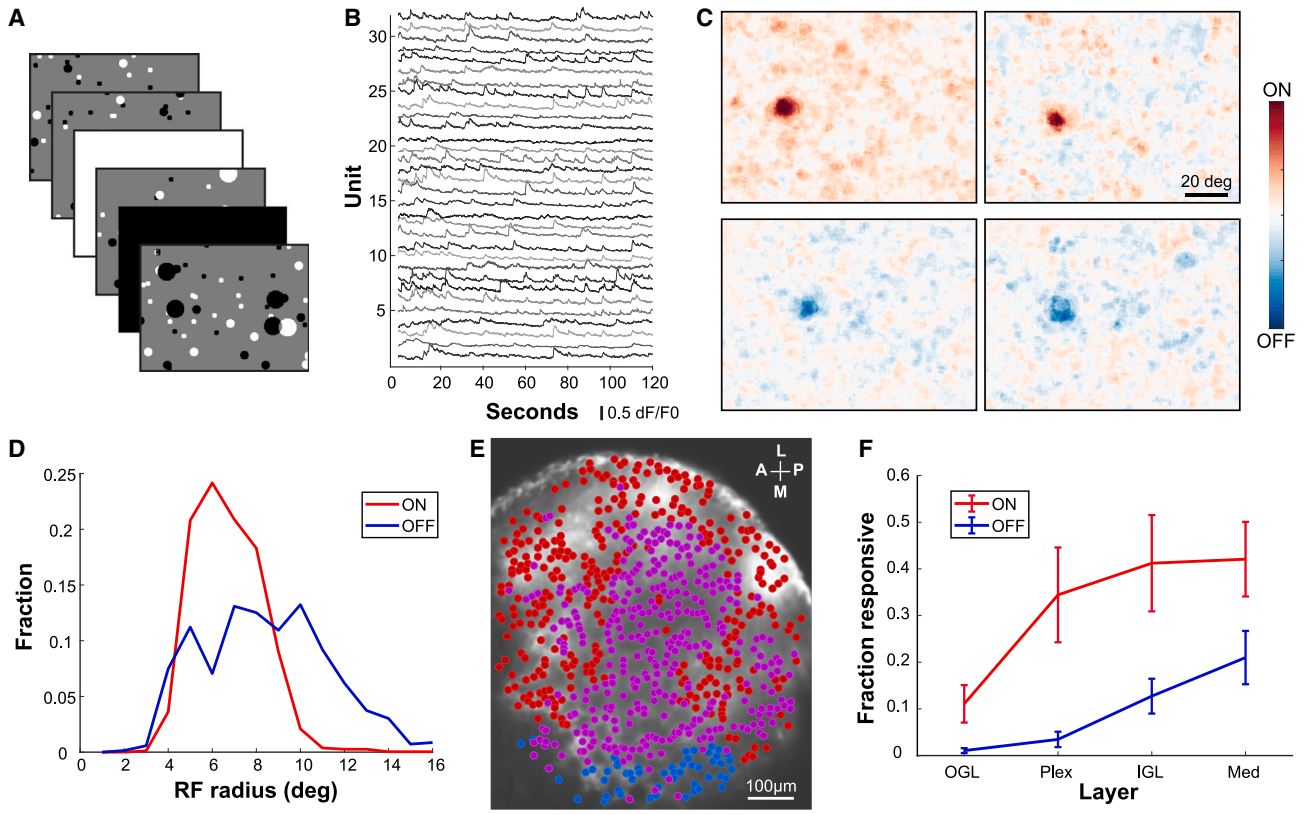

Figure 3. ON and OFF receptive fields mapped with a sparse noise stimulus

(A) Example frames from the sparse noise stimulus used to map receptive fields. Frames were presented consecutively in a randomized order for 1 s each.

(B) Traces of fluorescence activity at 32 locations across the optic lobe in response to the sparse noise stimulus.

(C) RFs from four example units, two each for ON (top) and OFF (bottom) components of the stimulus. Note that because these units are from within a single imaging field of view, the RFs are in the same vicinity of visual space, consistent with retinotopic organization.

(D) Histogram of RF sizes for ON and OFF stimuli (n = 6 animals).

(E) Location of units with RFs for ON (red), OFF (blue), or both (magenta) in one session across the optic lobe.

(F) Fraction of units overall with significant RFs for ON and OFF across the layers of the optic lobe (n = 6 animals).

See also Video S2.

Spatially localized ON and OFF receptive fields

We used a sparse noise stimulus adapted from Piscopo et al.[47] to calculate ON and OFF RFs. The stimulus consisted of frames of ON and OFF circular spots of three different sizes (radius = 3, 6, and 12 deg) in a randomly distributed pattern, along with randomly interleaved ON or OFF full-field frames (Figure 3A). Each frame was presented for 1 s over a total recording time of 10 min. This sparse noise stimulus elicited robust and spatially localized fluorescence responses across the optic lobe, as demonstrated in Figure 3B and Video S2.

For analysis, we selected individual regions of interest (ROIs), 20 × 20 μm, centered on peaks in the mean fluorescence image above a baseline fluorescence threshold, to exclude regions that were not loaded with calcium indicator. This identified ~500–1,000 ROIs spaced across each of the multiple layers of the optic lobe captured within each imaging field (e.g., Figure 3E). We selected this approach rather than extracting responses specifically from cell bodies as typically performed for calcium imaging in vertebrates, both due to the challenge in localizing signals to individual cells in tightly packed cell body layers and the fact that, in invertebrates, much of the neural signal is localized to processes within the neuropil. We refer to each ROI as a unit, denoting a specific location within the optic lobe rather than a single neuron. This analysis allowed us to map how visual information is represented at locations across the optic lobe. As noted in the discussion, single-cell or cell-type-specific recordings will likely be needed to directly probe individual cell tuning properties.

We computed RFs for each unit using reverse correlation based on the evoked dF/F0 fluorescence signal for each frame of the sparse noise stimulus, excluding the full-field flashes (STAR Methods). We performed this separately for the ON (light) and OFF (dark) components of the stimulus to avoid cancelation of positive and negative stimulus contrast for units that responded to both polarities. This revealed spatially localized RFs for both ON and OFF stimuli, as shown by examples in Figure 3C. RFs were generally circularly symmetric by visual inspection, so we fit RFs to a Gaussian model to determine their size and location within visual space. Across experiments, 59% ± 26% of all units had an RF significantly above background, as determined by their Z scored response. The Gaussian model provided a good fit to the RFs, with a pixel-wise correlation between the measured RF and model fit of 0.85 ± 0.07 for ON

Please cite this article in press as: Pungor et al., Functional organization of visual responses in the octopus optic lobe, Current Biology (2023), https://doi.org/10.1016/j.cub.2023.05.069

CellPress
OPEN ACCESS

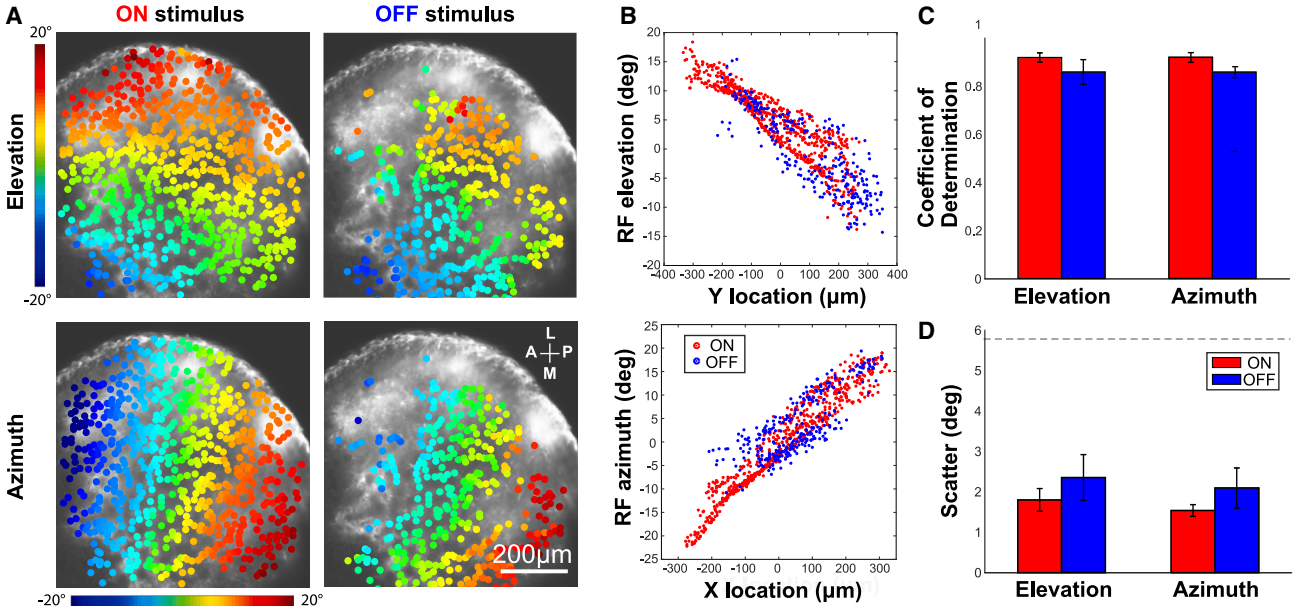

Figure 4. Retinotopic organization of visual responses in the octopus optic lobe

(A) Example mapping of RFs in the optic lobe of responses to both ON (left) and OFF (right) stimuli. Areas are colored by the position of their RFs along the elevation (top) and azimuth (bottom), as shown by the color scale bars (degrees of visual space). Based on the position of the octopus eyes, elevation corresponds to the dorsal-ventral axis of the animal's body, and azimuth corresponds to the anterior-posterior axis of the animal's body.

(B) Scatterplot of RF location for elevation (top) and azimuth (bottom) versus unit location within the optic lobe, for both ON and OFF responses. Adjacent groups of cells responded to adjacent areas of the visual field.

(C) Mean coefficient of determination for elevation and azimuth maps across all recordings (n = 6 animals).

(D) Mean scatter in RF location for elevation and azimuth, across all recordings (n = 6 animals). Dashed line shows chance level based on a shuffle control.

RFs and 0.74 ± 0.14 for OFF (mean ± SD). The lower correlation for OFF response likely reflects noisier RF estimates due to the lower response amplitude in OFF units (see Figure 4, below), but in both cases the vast majority of variance in the RF was explained by the Gaussian model. The RF radius, based on sigma of the Gaussian fit, was 5.7 ± 0.6 deg for ON and 7.4 ± 0.6 deg for OFF ($p = 0.31$ for ON versus OFF) (Figure 3D). Note that this is likely an overestimate of the RF size of individual neurons, as the response of each unit within the lobe represents the summed response of a number of individual neurons.

In each experiment, the measured RFs only subtended a restricted region of the visual field, consistent with a retinotopic organization and the fact that we are only imaging a limited extent of the optic lobe area (roughly 1/10th, as described above). We calculated that an area of 430 ± 290 deg^2 (mean ± SD) of the visual field that was covered by the RFs in each experiment. For context, the projection screen was 5,400 deg^2 (90 × 60 deg), so the fraction of visual space represented (~1/12th) corresponds well to the fraction of the optic lobe imaged.

We next examined the distribution of ON and OFF responses across the optic lobe to determine where the pathway for processing each arises. Figure 3E shows all units in an example recording labeled based on whether they had an RF for only ON (red), only the OFF (blue) component, or for both components of the stimulus (magenta). Although ON responses are distributed throughout the lobe, OFF responses are largely restricted to the deeper layers of the IGL and Med. To quantify this, we calculated the fraction of ON and OFF RFs in each layer across recordings (Figure 3F), confirming that OFF responses primarily emerge in the IGL and are strongest in the Med. The sequential emergence of OFF responses relative to ON is consistent with the fact that photoreceptor axons in cephalopods, which mainly terminate in the superficial layers of the optic lobe (Plex), respond to increments of light, and demonstrates that the OFF processing pathway originates in neurons further along the visual processing pathway.

We found both ON and OFF responses within the same fields of view, corresponding to the same region of visual space, suggesting that variations are primarily due to depth. However, it remains possible that there could also be variations in the ON/OFF distribution across the visual field in other regions of the optic lobe.

Retinotopic organization of the optic lobe

To determine whether there was a retinotopic organization of visually evoked responses in the octopus optic lobe, we labeled each unit according to the location of its RF, based on the center of the Gaussian fit described above. As shown in Figure 4A, we found clear retinotopic progression for ON and OFF responses along both the elevation and azimuth of the visual field, resulting in a map of visual space across the optic lobe. This is further demonstrated in Figure 4B, which shows the high degree of correlation between the unit's physical location across the optic lobe with its RF location in visual space. The retinotopic maps of ON and OFF RFs were also aligned in regions of the lobe that were responsive to both (Figure 4B). Note that, as described

Please cite this article in press as: Pungor et al., Functional organization of visual responses in the octopus optic lobe, Current Biology (2023), https://doi.org/10.1016/j.cub.2023.05.069

above, the imaged retinotopic map does not span the full visual space of the projector screen but is typically restricted to roughly 20 × 20 deg (mean 430 deg^2) due to the fact that we were only imaging a subregion of the optic lobe.

We next quantified the retinotopic organization in each experiment by performing a linear regression between the RF elevation/azimuth in the visual space of all responsive units and their x/y location within the optic lobe. We used both the x and y location of the units to predict each RF parameter, as the visual axes were not always aligned to the x and y axes of the imaging plane, depending on the orientation of the preparation. This fit resulted in a mean coefficient of determination greater than 0.8 for both ON and OFF maps across experiments (Figure 4C), confirming robust retinotopy. We also computed the scatter of RF locations (i.e., how much RF locations deviate from a linear retinotopic progression), based on the residuals from the fit, which demonstrated that individual units' RFs have a scatter of less than 2° (Figure 4D). Finally, the slope of the RF fit determines the magnification factor of the map (i.e., how much the RF location changes for a given distance in the brain), with a mean progression of 21.9 ± 1.4 μm/deg in elevation and 25.0 ± 3.0 μm/deg in azimuth. Together, these data provide the first functional demonstration of a retinotopic organization of visual information within the cephalopod brain.

Size selectivity in ON and OFF pathways across layers of the optic lobe

To further examine visual response properties and their organization within the octopus optic lobe, we next calculated size tuning of units based on their evoked responses to spots of different sizes in the sparse noise stimulus. For each unit with a significant RF, we determined the center of its ON or OFF RF from the Gaussian fit and computed the mean dF/F0 response time course when spots of different sizes appeared in this RF. We limited this analysis to units with significant RFs based on *Z* score, as described above, because it is only meaningful for units that have a defined RF location.

Figure 5A shows the mean time course of response during the 1-s stimulus presentation for each size stimulus, including full-field flash, for all units across experiments, divided into their layer within the optic lobe. In order to accurately represent the relative magnitude of responses across layers, given the differential distribution of ON and OFF units (Figure 3E), we weighted these mean traces by the respective fraction of responsive units within each layer. All responsive populations showed sustained activity throughout the 1 s stimulus presentation, although with diverse temporal dynamics. We note that because our measurements represent the activity of multiple neurons in each unit, these dynamics could also represent the summation of populations with heterogeneous temporal responses, for example, both transient and sustained responses.

For ON stimuli (Figure 5A, top), there was a strong and rapid response in the Plex, which was approximately equal in amplitude for all stimulus sizes, as well as to the full-field flashes. However, as responses progressed deeper into the IGL and Med, the sustained response increased for small stimuli but decreased for larger spots and full-field flashes, indicating size selectivity. Interestingly, the initial onset responses were similar across sizes, with the responses to different sizes diverging only after ~200 ms. Figure 5B shows the size tuning curve of ON responses for each layer, based on the mean dF/F0 across stimulus duration, normalized to the response to the smallest stimulus size. These show a decrease in the relative response to larger stimuli in the IGL and Med. Together, the responses to ON stimuli showed an emergence of size selectivity, both over time and across layers.

In contrast, responses to OFF stimuli (Figure 5A, bottom) only appeared in deeper layers of the optic lobe (IGL and Med). There was no size suppression across different sized spots, in contrast to what was seen in the ON. Rather, responses to OFF spots of all sizes were roughly equal, leading to a relative bias toward large stimuli in OFF compared with ON. Strikingly, there was no response at all to the full-field OFF stimulus, despite responses to the range of OFF spot sizes and to full-field ON. These differences in spatial integration for ON and OFF suggest that different processing pathways exist for these two luminance modalities, even in these early visual processing stages.

Finally, we examined the mean time course of response onset to ON and OFF spots across the layers of the optic lobe (Figures 5C and 5D), revealing distinct temporal dynamics. ON responses increased rapidly in the Plex, and then spread into the deeper regions of the IGL and Med. On the other hand, OFF responses were first seen predominantly in the Med (Figure 5A, bottom panels), and had a slower rise time (Figure 5C, blue trace). We quantified this difference in time course based on the mean rise time to half-maximum response (Figure 5D). It should be noted that this metric represents the rate of increase of response rather than latency to first response, which was faster than our framerate as clear responses were already seen in the first frame following stimulus onset (Figure 5C). There was an approximately 100-ms difference in rise time for ON responses from Plex to IGL and Med, and an additional 100 ms difference within the Med from ON responses to OFF responses (Figure 5D), consistent with a later emergence in the visual processing circuit.

DISCUSSION

Octopuses represent an intriguing independent evolution of a complex nervous system. However, relatively little is known about how their brain functions at the neural level. Combining large-scale two-photon calcium imaging with controlled visual stimuli, we were able to overcome technical challenges that previously hindered recordings of neural activity in cephalopods. The establishment of such recording techniques, and future improvements, will be essential for elucidating the computations performed in their visual system, as well as other aspects of sensory processing, cognition, and behavior in cephalopods.

Using this calcium imaging approach, we measured response properties of populations of neurons within the octopus optic lobe and began to identify what fundamental features of the visual world they encode and how these emerge in the early stages of visual processing. We found similarities in visual processing between octopus and other species, such as a retinotopic organization of responses, highlighting potential fundamental principles for the organization of visual systems across the animal kingdom. We also identified a unique organization of ON/OFF pathways and size selectivity, which may have arisen due to

Please cite this article in press as: Pungor et al., Functional organization of visual responses in the octopus optic lobe, Current Biology (2023), https://doi.org/10.1016/j.cub.2023.05.069

CellPress
OPEN ACCESS

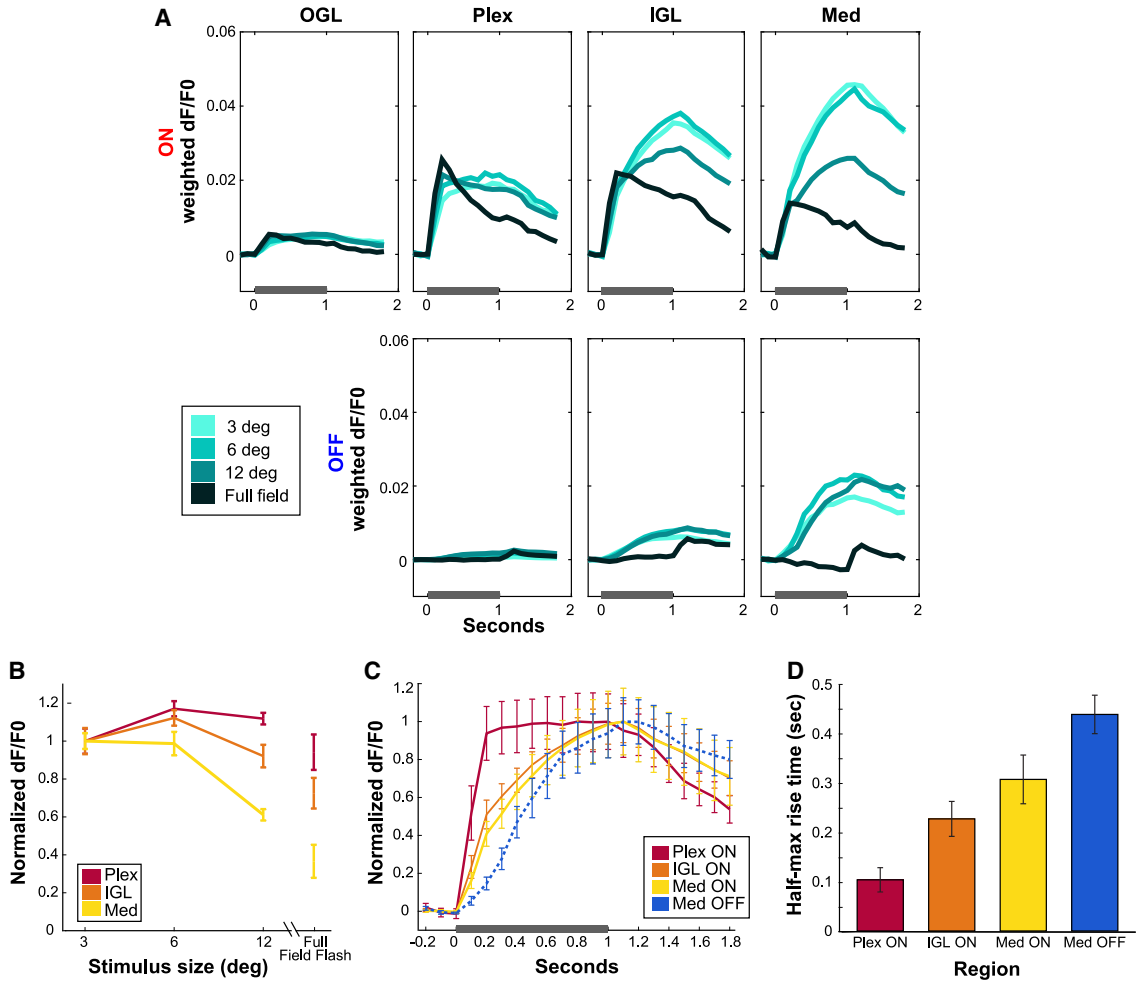

Figure 5. Size selectivity and temporal dynamics across the layers of the optic lobe

(A) Mean time course of ON (top) and OFF (lower) responses for each stimulus size, separated by layers of the optic lobe. Response for each layer and luminance are weighted by fraction of units responsive. OGL did not show a significant response to OFF and was omitted from this figure. Stimulus onset is at t = 0, and each frame was presented for 1 s, as shown by the gray bars on the x axis (n = 6 animals).

(B) Mean size tuning curves for ON responses in each layer, normalized to the response to the smallest stimulus (n = 6 animals).

(C) Mean time course of unit responses, averaged across the three sizes of stimulus spots and normalized to the maximum response, for ON (Plex, IGL, and Med) and OFF (Med) (n = 6 animals).

(D) Mean rise time to half-maximum response from data in (C).

these animals' environmental constraints[48] or distinct evolutionary trajectories.[49] These findings are the first to show visual processing dynamics across the layers of the octopus optic lobe and provide a foundation for studying the processing of more complex visual features.

Spatial organization of response properties in the optic lobe

Although there have been previous studies of the anatomical organization of the octopus visual system, little is known about its functional organization. Based on the fashion in which the optic nerves from the eye were found to enter the optic lobe,[16,50,51] it was predicted that visual information would be retinotopically organized within the lobe as it is in many, though not all,[42] visual systems across the animal kingdom. However, studies in the motor system of cephalopods demonstrated a surprising lack of somatotopy in their central brain, suggesting they may have evolved alternative, non-topographic architectures for representing spatial information.[52] In this study, we found that neural coding in the visual system of the octopus is indeed organized retinotopically, with aligned maps for responses to ON and OFF stimuli, demonstrating that the lack of topographic mapping previously observed in the motor system is not a general feature of cephalopod brain organization.

Previous anatomical studies had suggested potential neural circuits across the layers of the octopus optic lobe that could implement sequential processing of visual input,[13,14,16] as in the vertebrate retina or fly visual system.[53] Our findings support these predictions, demonstrating that the temporal dynamics of visual responses in octopuses do in fact proceed sequentially across the laminar organization of their brain. This is accompanied by a transformation of the visual input, including the

Please cite this article in press as: Pungor et al., Functional organization of visual responses in the octopus optic lobe, Current Biology (2023), https://doi.org/10.1016/j.cub.2023.05.069

emergence of the OFF pathway, as well as an increase in size selectivity in the ON pathway. Our findings of differential response dynamics across distinct layers provide an initial framework for understanding the functional computations performed by the cephalopod visual system.

Comparative aspects of ON/OFF pathways and spatial processing

A key computation for any visual system is the ability to respond to both light and dark stimuli within a scene. Given that photoreceptors depolarize to only ON (invertebrates) or OFF (vertebrates) stimuli, there is a necessary computation to invert the polarity of the photoreceptor signal within the subsequent visual circuitry to achieve this. For vertebrates, it is known that this inversion occurs at the photoreceptor to bipolar cell synapse,[54] while in *Drosophila* segregated ON and OFF responses emerge one synapse further from the photoreceptors, between the lamina and Med.[55]

Here, we found that ON responses dominate in the primary input layer of the octopus optic lobe, the Plex, corresponding to the fact that cephalopod photoreceptors depolarize to light increments. OFF responses only emerge initially in the IGL and are greatly increased in the Med, suggesting a potential site for the sign inversion circuitry. We also found that OFF responses have a strikingly different profile from ON. Despite prominent responses to full-field ON stimuli across layers, there is a complete lack of response to full-field OFF stimuli. This suggests that the OFF pathway may emerge through a different mechanism than direct inversion of the photoreceptor input, which would yield responses to a full-field OFF stimulus. One possibility is that the OFF pathway receives input from a subset of ON neurons that have completely suppressed the response to a full-field stimulus. A more intriguing possibility is that the mechanisms that generate OFF responses may rely directly on boundaries between light and dark regions, which would explain why OFF responses are driven by localized dark stimuli (i.e., spots) that contain such edges, but not full-field stimuli, which do not.

Additionally, we found differences in size selectivity for spots in the ON and OFF pathways (Figure 5A). Although responses in the ON pathway decreased for larger spots, the responses to spots in the OFF pathway were roughly equal across the sizes of stimuli we measured. This implies a net bias toward the enhancement of responses to smaller stimuli in the ON pathway. Asymmetries in ON/OFF visual processing have been found in other species across the animal kingdom and are thought to enhance ethologically relevant visual features to meet each animals' specific visual demands.[56–60] The enhancement of responses to smaller stimuli in the ON pathway that we observed may be beneficial when processing visual scenes underwater, where light intensity is greatly attenuated by both absorption and scatter.[61] As a result, nearby objects, like potential prey, would tend to appear bright against a large, dark background. An OFF pathway biased toward larger stimuli might also aid in the detection of large, looming objects, which often represent predators. It will be interesting to see whether such ON/OFF processing differences exist more broadly across cephalopods that occupy other ecological niches, particularly as these vary greatly in luminance levels and visual scene statistics.[62]

Implications for future studies

Our findings provide initial insight into how luminance and size information are processed within the different layers of the octopus optic lobe. However, both anatomical and transcriptomic studies[22,24,25,63] have revealed a high degree of cell type diversity within these layers, so the bulk response properties we examined here undoubtedly mask a high degree of underlying functional diversity. Identifying more detailed response properties within the parallel pathways of diverse cell types in this system will likely benefit from methods to record using genetically encoded calcium indicators, not yet available in cephalopods to date. Such an approach would also help address the challenge in associating activity in neural processes, which often dominate in invertebrate neurons, with individual neurons or populations of neurons.[64]

More broadly, future studies based on these findings and methodology could explore the range of feature selectivity in the visual system of octopuses, as has been studied in other species, such as motion processing, orientation selectivity, object recognition, and lateralization of visual responses.[65,66] Additionally, this approach can be used to study aspects of visual responses that may be specific to cephalopods, such as the ability to detect stimuli based on the polarization angle of light,[67] or to extract information from the visual scene for camouflage.[11] Further studies may continue to reveal how the cephalopod brain performs the computations that enable the remarkable visual capabilities of these enigmatic creatures.

STAR★METHODS

Detailed methods are provided in the online version of this paper and include the following:

- KEY RESOURCES TABLE
- RESOURCE AVAILABILITY
  - Lead contact
  - Materials availability
  - Data and code availability
- EXPERIMENTAL MODEL AND SUBJECT DETAILS
- METHOD DETAILS
  - Calcium imaging
  - Visual stimuli
- QUANTIFICATION AND STATISTICAL ANALYSIS
  - Data analysis
  - Statistical analysis

SUPPLEMENTAL INFORMATION

Supplemental information can be found online at https://doi.org/10.1016/j.cub.2023.05.069.

ACKNOWLEDGMENTS

We thank members of the Niell lab past and present for helpful discussions and comments on the manuscript and members of the Hochner lab (Hebrew University of Jerusalem) for advice on experimental methods for octopus. We thank the MBL Cephalopod Culture Program for supplying our experimental animals. We would also like to thank Damon Clark, Rhanor Gillette, Spencer Smith, and Michael Wehr for feedback on the manuscript. This work was supported by the National Institutes of Health R01NS118466-01, Office of Naval

Research N00014-21-1-2426, and Human Frontiers Science Program RPG0042/2019.

AUTHOR CONTRIBUTIONS

J.R.P. and C.M.N. conceived the project and designed experiments; J.R.P. led the project and performed experiments; V.A.A. and J.O.S.-C. both optimized the experimental protocol and performed experiments, contributing equally; C.M.N. and J.R.P performed data analysis; and all authors contributed to the writing of the manuscript.

DECLARATION OF INTERESTS

The authors declare no competing interests.

INCLUSION AND DIVERSITY

One or more of the authors of this paper self-identifies as an underrepresented ethnic minority in their field of research or within their geographical location. One or more of the authors of this paper self-identifies as a gender minority in their field of research. One or more of the authors of this paper self-identifies as a member of the LGBTQIA+ community. While citing references scientifically relevant for this work, we also actively worked to promote gender balance in our reference list.

Received: February 23, 2023
Revised: April 24, 2023
Accepted: May 30, 2023
Published: June 20, 2023

REFERENCES

1. Packard, A. (1972). Cephalopods and fish: the limits of convergence. Biol. Rev. *47*, 241–307.
2. Hanlon, R.T., and Messenger, J.B. (2018). Cephalopod Behaviour, Second Edition (Cambridge University Press).
3. Schnell, A.K., Hanlon, R.T., Benkada, A., and Jozet-Alves, C. (2016). Lateralization of eye use in cuttlefish: opposite direction for anti-predatory and predatory behaviors. Front. Physiol. *7*, 620.
4. Bidel, F., Bennett, N.C., and Wardill, T.J. (2022). Octopus bimaculoides' arm recruitment and use during visually evoked prey capture. Curr. Biol. *32*, 4780–4781.
5. Shashar, N., Rutledge, P., and Cronin, T. (1996). Polarization vision in cuttlefish in a concealed communication channel? J. Exp. Biol. *199*, 2077–2084.
6. Hanlon, R.T., Naud, M.J., Shaw, P.W., and Havenhand, J.N. (2005). Behavioural ecology: transient sexual mimicry leads to fertilization. Nature *433*, 212.
7. Karson, M.A., Jean, G.B., and Hanlon, R.T. (2003). Experimental evidence for spatial learning in cuttlefish (Sepia officinalis). J. Comp. Psychol. *117*, 149–155.
8. Alves, C., Boal, J.G., and Dickel, L. (2008). Short-distance navigation in cephalopods: a review and synthesis. Cogn. Process. *9*, 239–247.
9. Chiao, C.C., Ulmer, K.M., Siemann, L.A., Buresch, K.C., Chubb, C., and Hanlon, R.T. (2013). How visual edge features influence cuttlefish camouflage patterning. Vision Res. *83*, 40–47.
10. El Nagar, A., Osorio, D., Zylinski, S., and Sait, S.M. (2021). Visual perception and camouflage response to 3D backgrounds and cast shadows in the European cuttlefish, *Sepia officinalis*. J. Exp. Biol. *224*, jeb238717.
11. Reiter, S., and Laurent, G. (2020). Visual perception and cuttlefish camouflage. Curr. Opin. Neurobiol. *60*, 47–54.
12. Wells, M.J. (1962). The Brain and Behavior of Cephalopods (Stanford University Press).
13. Ramón y Cajal, S. (1930). Contribución al conocimiento de la retina y centros ópticos de los cefalópodos (Unión Internacional de Ciencias Biológicas, Comité Español).
14. Young, J.Z. (1960). Regularities in the retina and optic lobes of octopus in relation to form discrimination. Nature *186*, 836–839.
15. Young, J.Z. (1962). The optic lobes of Octopus vulgaris. Philos. Trans. R. Soc. Lond. *245*, 19–58.
16. Young, J.Z. (1971). The Anatomy of the Nervous System of Octopus Vulgaris (Oxford University Press).
17. Young, J.Z. (1974). The central nervous system of Loligo. I. The optic lobe. Philos. Trans. R. Soc. Lond. B Biol. Sci. *267*, 263–302.
18. Saidel, W.M. (1982). Connections of the octopus optic lobe: an HRP study. J. Comp. Neurol. *206*, 346–358.
19. Chung, W.S., Kurniawan, N.D., and Marshall, N.J. (2020). Toward an MRI-based mesoscale connectome of the squid brain. iScience *23*, 100816.
20. Williamson, R., and Chrachri, A. (2004). Cephalopod neural networks. Neurosignals. *13*, 87–98.
21. Liu, Y.C., Liu, T.H., Su, C.H., and Chiao, C.C. (2017). Neural organization of the optic lobe changes steadily from late embryonic stage to adulthood in cuttlefish Sepia pharaonis. Front. Physiol. *8*, 538.
22. Styfhals, R., Zolotarov, G., Hulselmans, G., Spanier, K.I., Poovathingal, S., Elagoz, A.M., De Winter, S., Deryckere, A., Rajewsky, N., Ponte, G., et al. (2022). Cell type diversity in a developing octopus brain. Nat. Commun. *13*, 7392.
23. Duruz, J., Sprecher, M., Kaldun, J.C., Al-Soudy, A.S., Lischer, H.E.L., van Geest, G., Nicholson, P., Bruggmann, R., and Sprecher, S.G. (2023). Molecular characterization of cell types in the squid Loligo vulgaris. eLife *12*, e80670. https://doi.org/10.7554/eLife.80670.
24. Songco-Casey, J.O., Coffing, G.C., Piscopo, D.M., Pungor, J.R., Kern, A.D., Miller, A.C., and Niell, C.M. (2022). Cell types and molecular architecture of the Octopus bimaculoides visual system. Curr. Biol. *32*, 5031–5044.e4.
25. Gavriouchkina, D., Tan, Y., Ziadi-Künzli, F., Hasegawa, Y., Piovani, L., Zhang, L., Sugimoto, C., Luscombe, N., Marlétaz, F., and Rokhsar, D.S. A single-cell atlas of bobtail squid visual and nervous system highlights molecular principles of convergent evolution. Preprint at bioRxiv. 10.1101/2022.05.26.490366.
26. Hamasaki, D.I. (1968). The ERG-determined spectral sensitivity of the octopus. Vision Res. *8*, 1013–1021.
27. Lange, G.D., and Hartline, P.H. (1974). Retinal responses in squid and octopus. J. Comp. Physiol. *93*, 19–36.
28. Land, M.F., and Fernald, R.D. (1992). The evolution of eyes. Annu. Rev. Neurosci. *15*, 1–29.
29. Moccia, F., Cristo, C.D., and Di Cosmo, A. (2009). Lost in phototransduction: a few facts and hypotheses on cephalopod photoresponse. Front. Biosci. (Schol Ed) *1*, 319–328.
30. Brown, P.K., and Brown, P.S. (1958). Visual pigments of the octopus and cuttlefish. Nature *182*, 1288–1290.
31. Messenger, J.B., Wilson, A.P., and Hedge, A. (1973). Some evidence for colour-blindness in Octopus. J. Exp. Biol. *59*, 77–94.
32. Marshall, N.J., and Messenger, J.B. (1996). Colour-blind camouflage. Nature *382*, 408.
33. Tasaki, K., Oikawa, T., and Norton, A.C. (1963). The dual nature of the octopus electroretinogram. Vision Res. *3*, 61–73.
34. Norton, A.C., Fukada, Y., Motokawa, K., and Tasaki, K. (1966). An investigation of the lateral spread of potentials in the octopus retina. Vision Res. *5*, 253–267.
35. Hartline, P.H., and Lange, G.D. (1974). Optic nerve responses to visual stimuli in squid. J. Comp. Physiol. *93*, 37–54.
36. Saidel, W.M., Shashar, N., Schmolesky, M.T., and Hanlon, R.T. (2005). Discriminative responses of squid (Loligo pealeii) photoreceptors to polarized light. Comp. Biochem. Physiol. A Mol. Integr. Physiol. *142*, 340–346.

37. Patterson, J.A., and Silver, S.C. (1983). Afferent and efferent components of octopus retina. J. Comp. Physiol. *151*, 381–387.

38. Boycott, B.B., Lettvin, J.Y., Maturana, H.R., and Wall, P.D. (1965). Octopus optic nerve responses. Exp. Neurol. *12*, 247–256.

39. Westheimer, G. (2007). The ON–OFF dichotomy in visual processing: from receptors to perception. Prog. Retin. Eye Res. *26*, 636–648.

40. Ichinose, T., and Habib, S. (2022). ON and OFF signaling pathways in the retina and the visual system. Front. Ophthalmol. (Lausanne) *2*, https://doi.org/10.3389/fopht.2022.989002.

41. Ryu, L., Kim, S.Y., and Kim, A.J. (2022). From photons to behaviors: neural implementations of visual behaviors in Drosophila. Front. Neurosci. *16*, 883640.

42. Fournier, J., Müller, C.M., Schneider, I., and Laurent, G. (2018). Spatial information in a non-retinotopic visual cortex. Neuron *97*, 164–180.e7.

43. Pickford, G.E., and McConnaughey, B.H. (1949). The octopus bimaculatus problem: A study in sibling species. Bull. Bingham Oceanogr. Collect. *12*, 1–66.

44. Albertin, C.B., and Simakov, O. (2020). Cephalopod biology: at the intersection between genomic and organismal novelties. Annu. Rev. Anim. Biosci. *8*, 71–90.

45. Niell, C.M., and Smith, S.J. (2005). Functional imaging reveals rapid development of visual response properties in the zebrafish tectum. Neuron *45*, 941–951.

46. Garaschuk, O., Milos, R.I., Grienberger, C., Marandi, N., Adelsberger, H., and Konnerth, A. (2006). Optical monitoring of brain function in vivo: from neurons to networks. Pflugers Arch. *453*, 385–396.

47. Piscopo, D.M., El-Danaf, R.N., Huberman, A.D., and Niell, C.M. (2013). Diverse visual features encoded in mouse lateral geniculate nucleus. J. Neurosci. *33*, 4642–4656.

48. Chung, W.S., and Marshall, N.J. (2017). Complex visual adaptations in squid for specific tasks in different environments. Front. Physiol. *8*, 105.

49. Grasso, F.W., and Basil, J.A. (2009). The evolution of flexible behavioral repertoires in cephalopod molluscs. Brain Behav. Evol. *74*, 231–245.

50. Saidel, W.M. (1979). Relationship between photoreceptor terminations and centrifugal neurons in the optic lobe of octopus. Cell Tissue Res. *204*, 463–472.

51. Chung, W.S., Kurniawan, N.D., and Marshall, N.J. (2022). Comparative brain structure and visual processing in octopus from different habitats. Curr. Biol. *32*, 97–110.e4.

52. Zullo, L., Sumbre, G., Agnisola, C., Flash, T., and Hochner, B. (2009). Nonsomatotopic organization of the higher motor centers in octopus. Curr. Biol. *19*, 1632–1636.

53. Sanes, J.R., and Zipursky, S.L. (2010). Design principles of insect and vertebrate visual systems. Neuron *66*, 15–36.

54. Dowling, J.E. (2012). The Retina: An Approachable Part of the Brain, Revised Edition (Harvard University Press).

55. Behnia, R., Clark, D.A., Carter, A.G., Clandinin, T.R., and Desplan, C. (2014). Processing properties of ON and OFF pathways for Drosophila motion detection. Nature *512*, 427–430.

56. Leonhardt, A., Ammer, G., Meier, M., Serbe, E., Bahl, A., and Borst, A. (2016). Asymmetry of Drosophila ON and OFF motion detectors enhances real-world velocity estimation. Nat. Neurosci. *19*, 706–715.

57. Clark, D.A., Fitzgerald, J.E., Ales, J.M., Gohl, D.M., Silies, M.A., Norcia, A.M., and Clandinin, T.R. (2014). Flies and humans share a motion estimation strategy that exploits natural scene statistics. Nat. Neurosci. *17*, 296–303.

58. Emran, F., Rihel, J., Adolph, A.R., Wong, K.Y., Kraves, S., and Dowling, J.E. (2007). OFF ganglion cells cannot drive the optokinetic reflex in zebrafish. Proc. Natl. Acad. Sci. USA *104*, 19126–19131.

59. Zhou, M., Bear, J., Roberts, P.A., Janiak, F.K., Semmelhack, J., Yoshimatsu, T., and Baden, T. (2020). Zebrafish retinal ganglion cells asymmetrically encode spectral and temporal information across visual space. Curr. Biol. *30*, 2927–2942.e7.

60. Mazade, R., Jin, J., Pons, C., and Alonso, J.M. (2019). Functional specialization of ON and OFF cortical pathways for global-slow and local-fast vision. Cell Rep. *27*, 2881–2894.e5.

61. Cronin, T.W., Johnsen, S., Justin Marshall, N., and Warrant, E.J. (2014). Visual Ecology (Princeton University Press).

62. Chung, W.S., and Marshall, N.J. (2016). Comparative visual ecology of cephalopods from different habitats. Proc. Biol. Sci. *283*, 20161346.

63. Young, J.Z. (1962). The optic lobes of Octopus vulgaris. Phil. Trans. R. Soc. Lond. B *245*, 19–58.

64. Strother, J.A., Nern, A., and Reiser, M.B. (2014). Direct observation of ON and OFF pathways in the Drosophila visual system. Curr. Biol. *24*, 976–983.

65. Byrne, R.A., Kuba, M.J., and Meisel, D.V. (2004). Lateralized eye use in Octopus vulgaris shows antisymmetrical distribution. Anim. Behav. *68*, 1107–1114.

66. Frasnelli, E., Ponte, G., Vallortigara, G., and Fiorito, G. (2019). Visual lateralization in the cephalopod mollusk octopus vulgaris. Symmetry *11*, 1121.

67. Shashar, N. (2014). Polarization vision in cephalopods. Polarized Light Polarization Vision Anim. Sci. 217–224. https://doi.org/10.1007/978-3-642-54718-8_8.

68. Fiorito, G., Affuso, A., Basil, J., Cole, A., de Girolamo, P., D'Angelo, L., Dickel, L., Gestal, C., Grasso, F., Kuba, M., et al. (2015). Guidelines for the care and welfare of cephalopods in research - a consensus based on an initiative by CephRes, FELASA and the Boyd Group. Lab. Anim. *49* (*Suppl*), 1–90.

69. Fiorito, G., Affuso, A., Anderson, D.B., Basil, J., Bonnaud, L., Botta, G., Cole, A., D'Angelo, L., De Girolamo, P., Dennison, N., et al. (2014). Cephalopods in neuroscience: regulations, research and the 3Rs. Invert. Neurosci. *14*, 13–36.

70. Koizumi, M., Shigeno, S., Mizunami, M., and Tanaka, N.K. (2018). Calcium imaging method to visualize the spatial patterns of neural responses in the pygmy squid, Idiosepius paradoxus, central nervous system. J. Neurosci. Methods *294*, 67–71.

71. McCormick, L.R., Levin, L.A., and Oesch, N.W. (2019). Vision is highly sensitive to oxygen availability in marine invertebrate larvae. J. Exp. Biol. *222*, https://doi.org/10.1242/jeb.200899.

72. Brainard, D.H. (1997). The psychophysics toolbox. Spat. Vis. *10*, 433–436.

Please cite this article in press as: Pungor et al., Functional organization of visual responses in the octopus optic lobe, Current Biology (2023), https://doi.org/10.1016/j.cub.2023.05.069

CellPress
OPEN ACCESS

STAR★METHODS

KEY RESOURCES TABLE

REAGENT or RESOURCE	SOURCE	IDENTIFIER
Chemicals, peptides, and recombinant proteins		
Cal520 AM ester	AAT Bioquest	Cat. #21130
Alexa Fluor 568 Hydrazide	Thermo Fisher	Cat. #A10437
Pluronic F-127 *20% solution in DMSO	AAT Bioquest	Cat. #20052
(R)-(−)-Phenylephrine hydrochloride powder	Sigma Aldrich	Cat. #P6126-5G
Agarose, low gelling temperature Type VII-A	Sigma Aldrich	Cat. # A0701-25G
Deposited data		
Calcium imaging data	Dryad	https://doi.org/10.5061/dryad.c2fqz61f2
Experimental models: Organisms/strains		
Octopus bimaculoides	Aquatic Research Consultants (San Pedro, CA)	N/A
Octopus bimaculoides	Cephalopod Culture Program (Woods Hole, MA)	N/A
Software and algorithms		
Matlab 2021b	Mathworks	www.mathworks.com/products/matlab; RRID: SCR_001622
Psychtoolbox	Brainard et al.[72]	www.psychtoolbox.org; RRID: SCR_002881
Scanbox	Neurolabware	https://www.scanbox.org/
Data analysis code	This paper	https://doi.org/10.5281/zenodo.7958768

RESOURCE AVAILABILITY

Lead contact

Further information and requests for resources and reagents should be directed to and will be fulfilled by the lead contact, Cristopher Niell (cniell@uoregon.edu).

Materials availability

This study did not generate new unique reagents.

Data and code availability

- Calcium imaging and receptive field data have been deposited at Dryad and are publicly available as of the date of publication. The DOI is listed in the key resources table.
- Original code to analyze calcium imaging data has been deposited at Zenodo and is publicly available as of the date of publication. The DOI is listed in the key resources table.
- Any additional information required to reanalyze the data reported in this paper is available from the lead contact upon request.

EXPERIMENTAL MODEL AND SUBJECT DETAILS

All studies were conducted with approved protocols from the University of Oregon Animal Care Services, in compliance with the Association for Assessment and Accreditation of Laboratory Animal Care International guidelines. Animal husbandry and protocols were carried out in accordance with published guidelines for the care and welfare of cephalopods in the laboratory.[68,69]

Octopus bimaculoides were obtained from the Cephalopod Culture Program at the Marine Biological Laboratory (Woods Hole, MA) and from Aquatic Research Consultants (Dr. Charles Winkler, San Pedro, CA). Animals used were 4–8 weeks old and of indeterminate gender. Octopuses were kept in a 250 gallon closed circulating seawater system, held at 22°C and illuminated on a 12/12hr day/night light cycle. Each animal was kept in an isolated enclosure within the system, allowing for ample freedom to roam, while keeping them

Please cite this article in press as: Pungor et al., Functional organization of visual responses in the octopus optic lobe, Current Biology (2023), https://doi.org/10.1016/j.cub.2023.05.069

isolated from potential cannibalism from counterparts. Each enclosure contained items that provided shelter (large shells, tubes) and environmental enrichment (smaller shells, Legos, beads, rotated weekly). Animals were fed a mixed diet of frozen shrimp, clams, and fish, offered daily.

METHOD DETAILS

Calcium imaging

Animals were deeply anesthetized in artificial seawater (ASW) (460mM NaCl2, 10mM KCl, 10mM glucose, 10mM HEPES, 55mM MgCl2, 11mM CaCl2, 2mM glutamine, pH 7.4) supplemented to contain 110mM MgCl2 at 13-15°C. When the animal was no longer responsive to a firm pinch test of the mantle, it was transferred to an oxygenated dish of a 30:70 mix of isotonic 370mM MgCl2 with ASW that was held between 13-15°C. Animals were then rapidly euthanized via decapitation and removal of the arm crown. A solution to dilate their pupils (10% phenylephrine HCl in ASW) was manually applied to the eyes. Dissection was performed to expose the brain and remove surrounding musculature and skin in order to reduce motion artifacts and increase optical access for recording.

The ex vivo preparation of the central brain and both eyes was secured to a coverslip using cyanoacrylate (Vetbond, 3M). A dye solution of 1mM Cal-520 AM (AAT Bioquest), 2.5% Alexa Fluor 568 Hydrazide (Thermo Fisher), 8% dimethylsulfoxide, and 2% pluronic acid (AAT Bioquest) in ASW was injected into one of the optic lobes via a glass micropipette needle (Harvard Apparatus Cat. Num. 30-0038) using a pressure injector (ASI). Micropipettes with a tip diameter of 9μm were back filled with the dye solution via capillary loading. For each animal, three individual injection sites were used. Three 1sec pulse injections at 5PSI pressure, with a constant 1PSI back pressure, were performed along the track of each injection site, with each injection done closer to the surface of the lobe than the last by retracting the needle ~50μm between each. Injections were targeted to the superficial layers (IGL and superficial medulla) of the optic lobe to optimize dye delivery to areas that were optically accessible in the imaging set-up. After injection, the preparation was covered in a thin layer of 4% low melt agarose in ASW (Sigma) to secure it and to minimize movement. This paradigm was adapted from previous work in zebrafish,[45] see also Koizumi et al.[70]

The preparation was kept in a recording chamber filled with ASW and continuously oxygenated via an airstone to maintain tissue viability.[71] The recording chamber consisted of a 7.6cmx7.6cmx5cm plastic box (TAP Plastics) where one side was replaced with a white diffusing glass (Edmund Optics, Cat. Num. 02-149) to serve as a projection screen for visual stimuli. The coverslip with the mounted preparation attached was secured to a custom-built rotatable platform within the recording chamber to allow for alignment of the preparation to the stimulus screen. The eye ipsilateral to the loaded dye was placed 2cm from the screen for recordings, with the contralateral eye facing away from the screen. The chamber temperature was monitored and held between 17-22°C.

Due to the need for the calcium indicator to be taken up into cells and then for the AM moiety to be cleaved, resulting in fluorescence, the preparation was kept in the dark under the two-photon microscope for 30-45 minutes before recording began. During this time we periodically examined the preparation for fluorescence and visual responses using a brief (<1sec) presentation of a flashing full field white stimulus. Experiments began after ~30-45 minutes, when the fluorescent loading had plateaued and visual responses were apparent.

Calcium imaging was performed with a two-photon microscope (Neurolabware), using a 16X Nikon CFI75 LWD objective, via the Scanbox software package for Matlab (MATHWORKS). Data were acquired at a 10Hz framerate, with an 800x800μm (796x796 pixel) field of view. Recordings were taken at 90 to 170μm depths from the dorsal surface of the optic lobe.

Visual stimuli

Custom generated visual stimuli, rendered using the PsychToolbox package for Matlab,[72] were displayed with a pico LCD projector (AAXA Technologies) onto the diffusing glass on the side of the recording chamber. To avoid light from the stimulus entering the two-photon detection pathway, the projected light was passed through a 450/50 bandpass filter (Chroma Technology Corporation), avoiding overlap with the emission spectrum of the Cal-520 calcium dye and the bandpass 525/50 emission filter of the microscope. The stimulus bandpass filter also restricted the stimulus light to be within the known absorption spectrum of cephalopod photopigments.[26] Stimuli were gamma-corrected in software and presented at 60FPS.

ON and OFF stimuli were presented as full contrast increments and decrements of light on a 50% luminance gray background. Initial mapping was performed using a stimulus consisting of full contrast ON (100% luminance) and OFF (0% luminance) rectangular spots (24x18deg) on a 6x4 grid spanning the projection screen, presented in a random order for a one second duration, for a total recording time of 5min. This stimulus was also repeated at the end of the experimental session to confirm stability and viability of the preparation. Full RF mapping was performed using a sparse noise stimulus, consisting of white and black spots (radius = 3, 6, 12 deg; density = 10%) on a gray (50% luminance) background, along with full-field white or black on 2% of frames. Each stimulus frame was presented for 1sec in a randomized order for a total duration of 10min. Preparations were kept in the dark for 10min between each stimulus set presentation. The results of presenting each stimulus set once to each of six animals are shown here. In some preparations additional stimuli were presented at the same or other recording locations but are not included in this study. Recordings reported here were taken 2-5.5 hours after injection.

Please cite this article in press as: Pungor et al., Functional organization of visual responses in the octopus optic lobe, Current Biology (2023), https://doi.org/10.1016/j.cub.2023.05.069

QUANTIFICATION AND STATISTICAL ANALYSIS

Data analysis

Data analysis was performed using custom software in MATLAB. We applied a rigid alignment of imaging data using the *sbxalign* function in Scanbox (Neurolabware). In order to detect large movements that were not corrected by the alignment algorithm, for each frame we calculated the pixel-wise correlation coefficient to the mean image. Frames with less that 90% correlation were discarded from further analyses.

We calculated the fluorescence activity (dF/F0) at each pixel as the standard (F(t) - F0) / F0, where F(t) is the fluorescence intensity of the pixel on each frame and F0 is the median fluorescence intensity of the pixel across the recording. To analyze local responses, we defined "units" as a 20μmx20μm wide square window, centered on local peaks within the mean fluorescence that were above the background fluorescence, to ensure that only areas with sufficient dye loading were analyzed. dF/F0 for each unit was calculated as the mean dF/F0 across pixels within the unit. Units were manually assigned to anatomical layers (OGL, IGL, Plex, and Med) based on location within the mean fluorescence image from the recording session.

To analyze receptive fields (RFs), based on the sparse noise stimulus, we first calculated the evoked response, $r(t)$, for each frame as the mean dF/F0 across the one second duration of stimulus presentation, minus the mean dF/F0 in the preceding 300msec. RFs were calculated by reverse correlation between the each stimulus frame, $s(x,y,t)$, and the evoked response to that frame.

$$RF(x,y) = \sum_t s(x,y,t) * r(t) \Big/ \sum_t r(t)$$

We computed the z-score for each RF based on the maximum absolute value of the RF, divided by the standard deviation across pixels. We used a z-score of 5.5 as the threshold for significant responses.

In order to analyze RF size and location, we fit each RF to a Gaussian function, defined as

$$RF_{fit}(x,y) = A * exp\left((x - x_0)^2 \Big/ 2\sigma_x^2 + (y - y_0)^2 \Big/ 2\sigma_y^2\right) + B$$

We used x_0, y_0 as the receptive field center, and computed RF radius as $(\sigma_x+\sigma_y)/2$. To quantify topographic maps, we performed a linear regression for each recording for responses to both azimuth and elevation, as a function of each unit's location within the optic lobe from the Gaussian fit, and used the coefficient of determination and standard deviation of residuals (scatter) as metrics of retinotopy.

Statistical analysis

Statistical tests for comparison of responses across populations within the optic lobe were performed using a t-test. To account for the nested design (many units per recording) of this analysis, all statistical tests were performed at the level of recordings, rather than total number of units recorded. Summary statistics in text and figures are presented as mean +/- standard error, unless otherwise noted.